Journal of Nuclear Materials 380 (2008) 93–98

Contents lists available at ScienceDirect

Journal of Nuclear Materials

journal homepage: www.elsevier.com/locate/jnucmat

# Structural modifications in pyrochlores caused by ions in the electronic stopping regime

M.K. Patel [a,d,*], V. Vijayakumar [a], S. Kailas [b], D.K. Avasthi [c], J.C. Pivin [d], A.K. Tyagi [e]

[a] High Pressure Physics Division, Bhabha Atomic Research Centre, Trombay, Mumbai 400 085, India
[b] Physics Group, Bhabha Atomic Research Centre, Trombay, Mumbai 400 085, India
[c] Inter-University Accelerator Center, Post Box No. 10502, Aruna Asaf Ali Marg, New Delhi 110 067, India
[d] CSNSM, IN2P3-CNRS, Batiment 108, 91405 Orsay Campus, France
[e] Chemistry Division, Bhabha Atomic Research Centre, Trombay, Mumbai 400 085, India

ARTICLE INFO

*Article history:*
Received 9 January 2008
Accepted 21 July 2008

*PACS:*
61.80.Jh
61.82.Ms
64.60.Cn
64.60.Kb
79.20.Rf
81.30.Hd

ABSTRACT

Damage caused by swift heavy ions with three different electronic stopping powers (120 MeV $Au^{9+}$ (22 keV/nm), 90 MeV $I^{7+}$ (17 keV/nm) and 70 MeV $Ni^{5+}$ (11 keV/nm)) in three pyrochlores ($Gd_2Zr_2O_7$, $Nd_2Zr_2O_7$ and $Gd_2Ti_2O_7$) with progressively increasing radius ratios ($r_A/r_B$ of $A_2B_2O_7$) of cations is reported. Since $I^{+7}$ is one of the ions used, these measurements also simulate fission fragment damage in pyrochlores and identify a potential host lattice for inert matrix fuel. X-ray diffraction on the irradiated materials indicate amorphization in $Gd_2Ti_2O_7$ at the lowest $S_e$ used, and a transition to anion-deficient fluorite ($Fm\bar{3}m$) structure with about 1% decrease in volume in $Nd_2Zr_2O_7$ and $Gd_2Zr_2O_7$ at higher $S_e$. In $Nd_2Zr_2O_7$ this is followed by amorphization and $Gd_2Zr_2O_7$ does not amorphize even at the highest $S_e$ employed. Raman analysis of $Gd_2Zr_2O_7$ and $Nd_2Zr_2O_7$, indicate an increase of Zr coordination number after irradiation and the bands become broader due to disordering. Analysis of the results shows that the radiation susceptibility of these pyrochlores in the electronic stopping regime strongly depends on the radius ratio of A to B cations and hence on the energy required for formation of cation antisites and anion Frenkel pairs, similar to their susceptibility in the nuclear stopping regime.

Published by Elsevier B.V.

## 1. Introduction

One of the most critical concerns in nuclear technology today is the disposal of high level nuclear waste (HLW), containing radiotoxic minor actinides (MA) ($^{239}Pu$, $^{241}Am$, $^{237}Np$, $^{244}Cm$, etc.) [1,2]. One of the methods proposed to reduce the amount of HLW significantly is partitioning and transmutation. This involves, first separating the MA from HLW (partitioning) and then reducing their quantity by further irradiation in existing reactors or in accelerator driven sub-critical systems (transmutation). To avoid the formation of new actinides, the partitioned MA should be incorporated into a matrix, with a low neutron capture cross-section, known as inert matrix fuel (IMF). In addition to this, the inert matrix should be non-toxic, have high melting point, good thermal conductivity, and most importantly very high radiation resistance [3,4].

An IMF or transmutation target, in a radiation environment, will experience large damaging due to neutrons, fission fragments (FF), α-particles and recoils produced during α-decay (α-recoils). FF's are mainly ions between Ga ($A = 69.72$) and Dy ($A = 162.5$) with energies in the range of 70–120 MeV. These ions interact with the target electrons and lose energy either by ionization or excitation of target atoms, contrary to ions of energy lower than 100 keV/amu which lose their energy mainly by colliding with atoms, resulting in a displacement cascade. FF's deposit a high density of energy within narrow cylindrical volumes around the ion path (called tracks), causing large pressure and temperature rises transiently, liable to result in structural transformations [5–8]. One major difference in damage caused by ions in the nuclear and electronic stopping regime is that damage creation in the first regime is by accumulation of Frenkel pairs while in the second formation of dislocation loops is a common mode of damage creation. Swift heavy ion (SHI) beams produced by accelerators can be used to simulate the damage caused by FF's outside reactors.

Recently, zirconate pyrochlores were envisaged as transmutation targets [9]. Pyrochlores have an excellent ability to accommodate several MA at the A site. Various studies indicate that they are highly resistant to damaging by α-decay [2,10]. Due to these

* Corresponding author. Address: High Pressure Physics Division, Bhabha Atomic Research Centre, Trombay, Mumbai 400 085, India. Tel.: +91 22 25593316; fax: +91 22 28906815.
*E-mail address:* maulikrk@gmail.com (M.K. Patel).

0022-3115/$ - see front matter Published by Elsevier B.V.
doi:10.1016/j.jnucmat.2008.07.007

**Table 1**
Radius ratio [13], cation antisite defect energy $E_{CA}$ (eV) [19], 48f oxygen '*x*' parameter [15] and O–D transformation temperature [20]

| Sample | $r_A/r_B$ | $E_{CA}$ (eV) | 48f '*x*' parameter | $T_{O-D}$ (°C) |
|---|---|---|---|---|
| $Gd_2Zr_2O_7$ | 1.46 | 3.20–3.60 | 0.345 | 1530 |
| $Nd_2Zr_2O_7$ | 1.54 | 4.00–4.40 | 0.334 | 2300 |
| $Gd_2Ti_2O_7$ | 1.75 | 5.60–6.00 | 0.326 | No transformation |

reasons they are being contemplated as potential host lattices for disposal of MA.

Assessment of the damage caused in pyrochlores by SHI's in the electronic stopping regime is sparse [9], unlike in the nuclear stopping regime [1–3,11,10]. For a detailed review on the radiation damage in pyrochlores in the nuclear stopping regime refer to a review of Ewing et al. [10] The present paper reports the results of an investigation of the radiation stability of pyrochlores under SHI irradiation and its dependence on ion beam and material parameters. Three pyrochlores with $r_A/r_B$ ratio in the two extreme limits ($Gd_2Zr_2O_7$ and $Gd_2Ti_2O_7$) and in the middle ($Nd_2Zr_2O_7$) of the pyrochlore stability region and with comparable physical properties (Table 1) were selected for this investigation.

## 2. Experimental

AR Grade $Gd_2O_3$, $Nd_2O_3$, $ZrO_2$ and $TiO_2$ powders were heated overnight to remove moisture and other volatile impurities. Stoichiometric amounts of reactants were mixed to get the required compositions. The products $Gd_2Zr_2O_7$, $Nd_2Zr_2O_7$ and $Gd_2Ti_2O_7$ were obtained by standard solid-state route. This included five steps heating at 1400–1500 °C for 24–36 h in air with intermittent grinding. Heating and cooling rates were kept at 2°/min. Powder XRD analysis confirmed the formation of the three pyrochlores. The powders were pelletized and sintered in the form of buttons of 8 mm diameter and 2 mm thickness. These pellets were irradiated with 120 MeV $Au^{9+}$, 90 MeV $I^{7+}$ and 70 MeV $Ni^{5+}$, each at various fluences ranging from $1 \times 10^{16}$ to $1 \times 10^{18}$ ions/m$^2$. The electronic stopping powers ($S_e$) of these ion beams in the three pyrochlores were estimated using SRIM 2003 [12] and are tabulated in Table 2. Fluences used in the present experiments are sufficient for the tracks to overlap. $I^{7+}$ ions (90 MeV) were used because their $Z$ and $S_e$ especially suits to simulate the effect of FF's. Ni and Au ions were used to assess the effect of the variation in $S_e$ on the structural stability of these materials. The irradiations were carried out using the 13UD Pelletron accelerator facility at the Inter-University Accelerator Centre (IUAC), New Delhi. Ion flux were less than $3 \times 10^{14}$ ions m$^{-2}$ s$^{-1}$. All irradiations were carried out at room temperatures under a vacuum of $10^{-6}$ torr. X-ray diffraction (XRD) measurements were done using the Bruker D8-Advance diffractometer at IUAC. The minimum projected range of these ions in pyrochlores is ≈10 μm, while the X-ray penetration depth in these materials is less than 4 μm and $S_e$ is dominant in this region. Hence, wide incidence could be used in XRD to assess the structural damage. The Cu Kα (0.15406 nm) radiation was used with a tube operated at 40 kV and 40 mA. The data were collected in $2\theta$ range between 20° and 80° with 0.02° steps using a position sensitive Ventic-1 detector. Raman spectra were recorded in backscattering geometry with a Renishaw single monochromator equipped with a CCD detector. The excitation source was the 488 nm line of an Ar-ion laser.

**Table 2**
Electronic energy loss (keV/nm) calculated using SRIM 2003 [12]

| Sample | 120 MeV Au | 90 MeV I | 70 MeV Ni |
|---|---|---|---|
| $Gd_2Zr_2O_7$ | 22.2 | 17.2 | 11.5 |
| $Nd_2Zr_2O_7$ | 20.9 | 16.2 | 10.8 |
| $Gd_2Ti_2O_7$ | 22.7 | 17.7 | 11.8 |

## 3. Results and discussion

The pyrochlore structure ($A_2^{3+}B_2^{4+}O_6$ Ò, Space group (S.G.) $Fd\bar{3}m$) is a derivative of the fluorite structure ($MX_2$, S.G. $Fm\bar{3}m$), but with two different cations and one eighth fewer anions. The atoms A, B, O, Ò occupy 16d, 16c, 48f and 8b sites, respectively. The larger $A^{3+}$ cation is eight oxygen coordinated with six 48f and two 8b oxygen anions, forming a distorted cubic polyhedron. The smaller $B^{4+}$ cation is coordinated with six oxygen in a distorted octahedron. There are two unique oxygen sites namely 48f, coordinated to two $B^{4+}$ cations and two $A^{3+}$ cations and the 8b which is tetrahedraly coordinated with only $A^{3+}$ cations. An unoccupied interstitial site 8a is surrounded by four $B^{4+}$ cations and the vacancy at the 8a site is ordered on the anion sublattice in pyrochlore and disordered in defect fluorite structure [13]. The pyrochlore structure is completely described by the cubic lattice parameter '*a*' and the 48f oxygen position parameter '*x*' and is identified by weak super lattice lines in the XRD pattern.

Structural modifications, monitored by XRD are shown in Figs. 1–4. The circled peaks in the spectra of unirradiated samples are superstructure peaks and are unique to the pyrochlore structure. It is observed that in $Gd_2Zr_2O_7$ and $Nd_2Zr_2O_7$, these peaks disappear (Figs. 1 and 2), indicating within XRD limits, a complete transformation from pyrochlore to anion-deficient fluorite (order–disorder) structure. $Nd_2Zr_2O_7$ is finally amorphized at $5 \times 10^{17}$ ions/m$^2$ on irradiation with 90 MeV $I^{7+}$ and 120 MeV $Au^{9+}$. $Gd_2Ti_2O_7$ is amorphized by ions with the lowest $S_e$ employed. It is also observed from Fig. 1 that with the increase in $S_e$ of ions, for the same fluence, there is a large broadening and a decrease in the intensity of diffraction peaks of $Gd_2Zr_2O_7$. The $S_e$ of a given ion species in the three pyrochlores is almost the same ≈16–17 keV/nm. It is quite clear that as $r_A/r_B$ increases from $Gd_2Zr_2O_7$ to $Nd_2Zr_2O_7$ to $Gd_2Ti_2O_7$ (Table 1), resistance to amorphization decreases. Similar observation is also made for 120 MeV Au and 70 MeV Ni ions. Also the significant increase in the amorphization efficiency with the $S_e$, which is found when comparing the intermixtures of diffraction peaks for a same value of deposited energy density ($S_e\,\phi$) ($\phi$ being the fluence). This effect testifies for the existence of a threshold in $S_e$ for damaging.

Fig. 4 shows that the (220) diffraction peak of $Nd_2Zr_2O_7$ irradiated with 70 MeV $Ni^{5+}$ shifts towards lower *d*-values. The initial *d*-values for (220) are very close to those in the ASTM files, and then the lattice shrinks upon irradiation. A similar effect was observed for $Gd_2Zr_2O_7$. The volume contraction observed is of about 1% for both these compounds. A similar result is obtained after irradiation with 90 MeV $I^{7+}$ and 120 MeV $Au^{9+}$ but at lower fluence. This is consistent with the calculations done by Rushton et al. [14] which yield a comparable volume decrease in $Gd_2Zr_2O_7$ and $Nd_2Zr_2O_7$ during transformation from a pyrochlore to defect fluorite structure associated with irradiation process in the nuclear stopping regime. Interestingly, it is also observed in the electronic stopping regime.

To obtain complementary information regarding the above observed order–disorder transformation, Raman scattering investigations were carried out. Factor group analysis of ($A_2^{3+}B_2^{4+}O_6$ Ò, S.G. $Fd\bar{3}m$) pyrochlores predicts the appearance of six Raman active modes [15],

$$\Gamma_{op} = A_{1g} + E_g + 4T_{2g}.$$

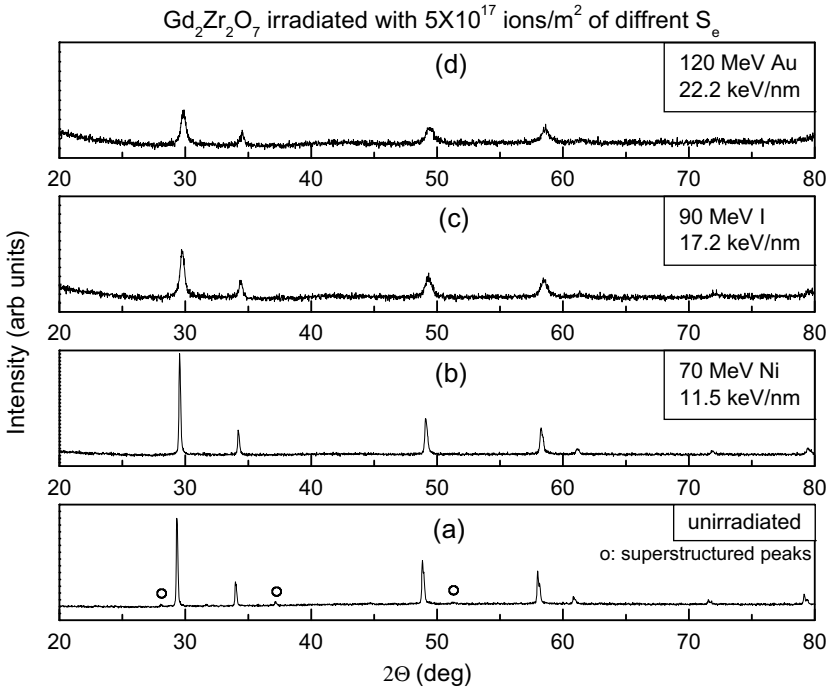


**Fig. 1.** XRD patterns of $Gd_2Zr_2O_7$, virgin and irradiated at fluence of $5 \times 10^{17}$ ions/m$^2$ with ions of variable electronic energy loss. (a) Virgin; (b) $S_e = 11.5$ keV/nm; (c) $S_e = 17.2$ keV/nm; (d) $S_e = 22.2$ keV/nm.

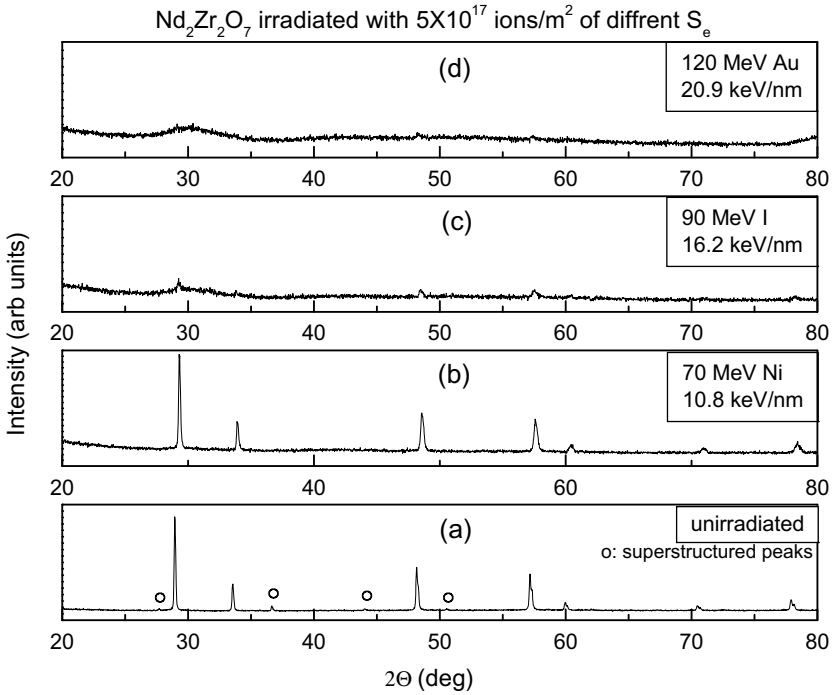


**Fig. 2.** XRD patterns of $Nd_2Zr_2O_7$ virgin and irradiated at fluence of $5 \times 10^{17}$ ions/m$^2$ with ions of variable electronic energy loss. (a) Virgin; (b) $S_e = 10.8$ keV/nm; (c) $S_e = 16.2$ keV/nm; (d) $S_e = 20.9$ keV/nm.

Fig. 5 shows Raman spectra of $Gd_2Zr_2O_7$, pristine and irradiated with $2.4 \times 10^{17}$ ions/m$^2$ Au ions of 120 MeV. Raman bands of the pristine sample, at 320, 400, 532 and 596 cm$^{-1}$, are due to one O–Gd–O bending ($E_g$), one Zr–O ($T_{2g}$) and two Gd–O ($A_{1g}$,$T_{2g}$) stretching modes, respectively [16]. The broad band observed near 700 cm$^{-1}$ is due to the Zr–$O_7$ ($T_{2g}$) species [17], accounting for the existence of defects (interstitial oxygen on the 8a site), because this compound is hardly obtained with a perfect pyrochlore structure. Upon irradiation with fluences ranging from $1 \times 10^{16}$ to $2.4 \times 10^{17}$ ions/m$^2$, this broad $T_{2g}$ band at 700 cm$^{-1}$ shifts towards lower frequencies and its intensity increases, indicating a monotonic increase in the number of Zr ions with a coordination near to 8, which is a characteristic of a fluorite lattice. An increase in the coordination number leads to an increase in Zr–O bond length

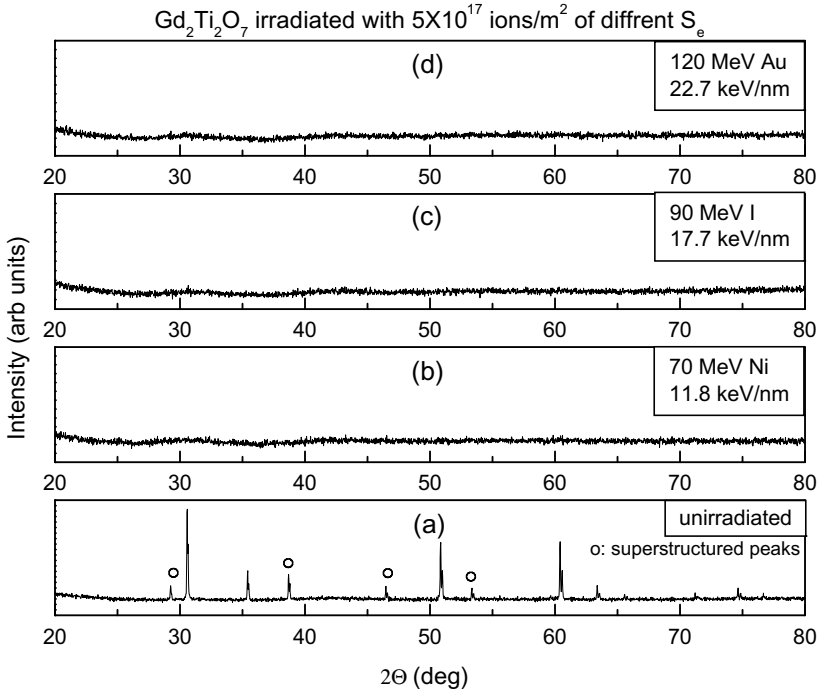


**Fig. 3.** XRD patterns of $Gd_2Ti_2O_7$ virgin and irradiated at fluence of $5 \times 10^{17}$ ions/m$^2$ with ions of variable electronic energy loss. (a) Virgin; (b) $S_e$ = 11.8 keV/nm; (c) $S_e$ = 17.7 keV/nm; (d) $S_e$ = 22.7 keV/nm.

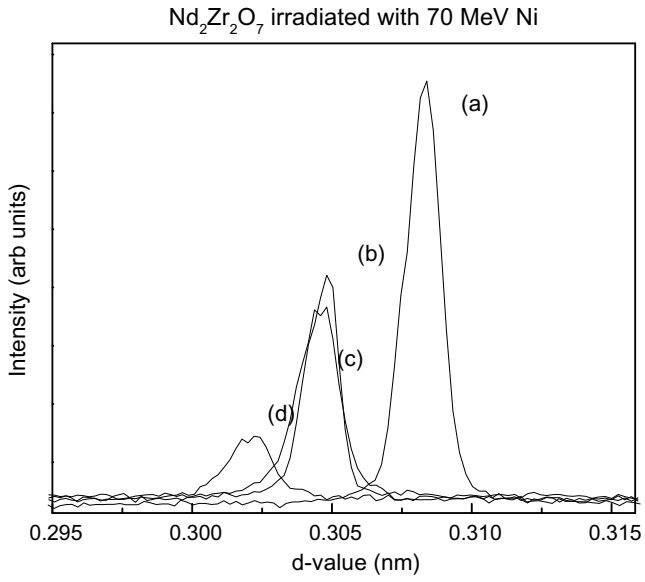


**Fig. 4.** Shift in the (220) diffraction peak towards lower $d$-values in $Nd_2Zr_2O_7$ irradiated 70 MeV Ni at various fluences. (a) Virgin; (b) $1 \times 10^{17}$ ions/m$^2$; (c) $5 \times 10^{17}$ ions/m$^2$; (d) $1 \times 10^{18}$ ions/m$^2$ (uncertainity in the analysis being ±0.0002 Å).

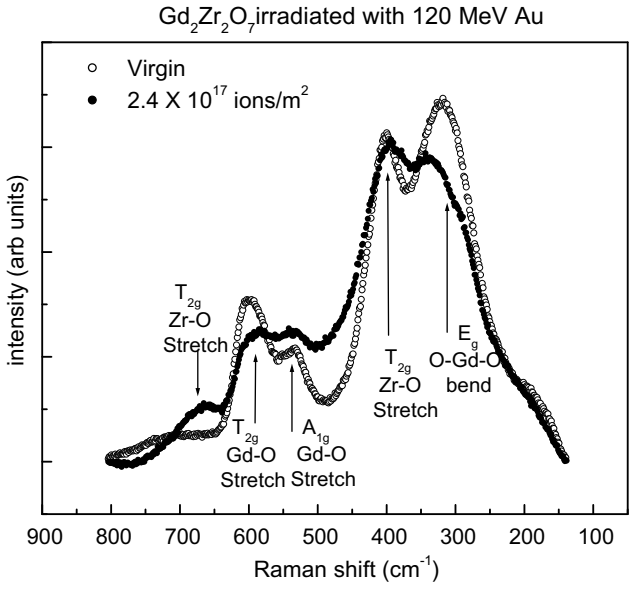


**Fig. 5.** Raman spectra of $Gd_2Zr_2O_7$, (while circles) virgin and (black circles) irradiated with $2.4 \times 10^{17}$ ions/m$^2$ of 120 MeV Au ions.

in the $ZrO_6$ polyhedra and the shift of $T_{2g}$ band to lower frequency. Irradiation also causes a broadening of other bands (Fig. 5). The $E_g$ mode shifts towards high frequencies with increase in the ion fluence while the $A_{1g}$ almost disappears. Since there are only 7 oxygen atoms, the vacancy at 8a sites become randomly distributed. This random distribution of defects suppresses the translation symmetry in anion-deficient fluorite and the selection rule ($k$ = 0) is no longer applicable, hence the Raman peaks become very broad. Thus, the changes in the vibrational modes confirms a transformation from ordered pyrochlore to disordered anion-deficient fluorite in $Gd_2Zr_2O_7$. Similar observations are also made for $Nd_2Zr_2O_7$ irradiated with 70 MeV Ni ions (Fig. 6(a)). But the Raman spectra of $Nd_2Zr_2O_7$ (Fig. 6(b)) show the disappearance of almost all the bands upon irradiated with 120 MeV Au, signifying the complete amorphization of this compound.

Since $r_A/r_B$ increases in the order $Gd_2Zr_2O_7$, $Nd_2Zr_2O_7$ and $Gd_2Ti_2O_7$, it is obvious that the structural stability has a strong dependence on $r_A/r_B$, apart from other material properties. Present results show that in the electronic stopping regime the stability follows the same trend as reported previously in the case of nuclear stopping regime [18,19]. In the following, we will first examine

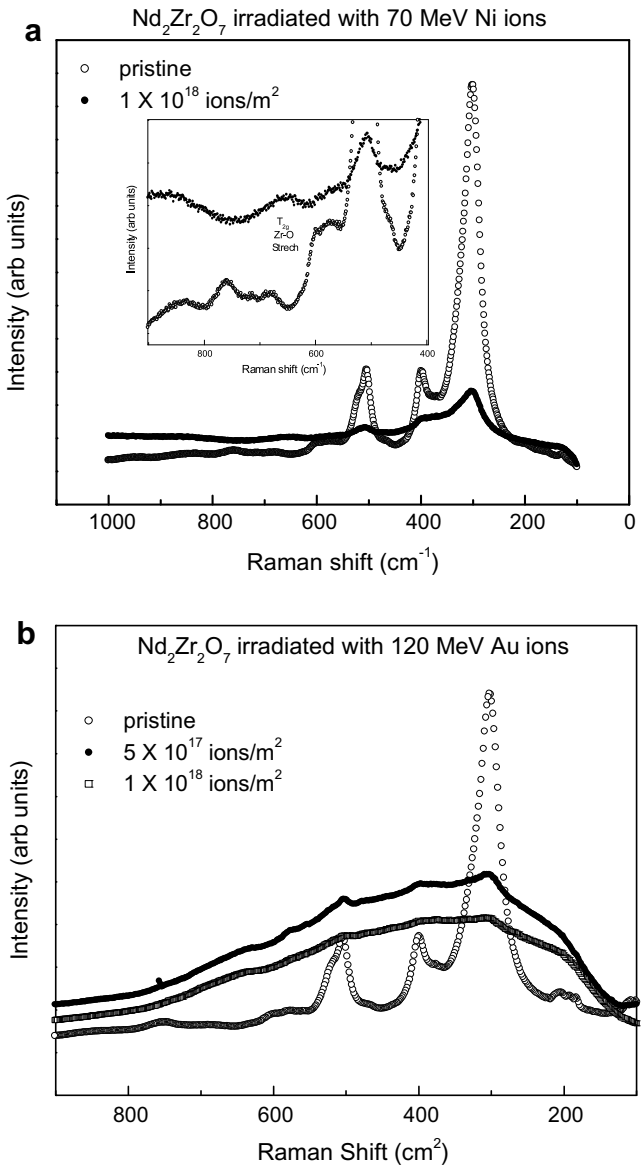


**Fig. 6.** Raman Spectra of $Nd_2Zr_2O_7$, (a) irradiated with 70 MeV Ni, (white circle) pristine and (black circle) $1 \times 10^{18}$ ions/$m^2$ and (b) irradiated with 120 MeV Au, (white circle) pristine, (black circle) $5 \times 10^{17}$ ions/$m^2$ and (white squares) $1 \times 10^{18}$ ions/$m^2$.

the structural aspects and then the other factors responsible for this behaviour.

Ordered pyrochlores generally exist with $r_A/r_B$ ranging from ≈1.36 to 1.76 [13]. The degree of ordering decreases with the decrease in $r_A/r_B$ (existence of $ZrO_7$ coordination in $Gd_2Zr_2O_7$), the pyrochlore gradually becoming anion-deficient fluorite [18,19]. The pyrochlore to anion-deficient fluorite, order–disorder transformation is brought about by site exchange of A and B cations (antisites) and relocation of the oxygen ion vacancy, which may be linked to the formation of a Frenkel pair since some B cations have a new interstitial O neighbour.

The radiation stability of oxide compounds with a structure related to the fluorite structure (pyrochlores and δ phases) in the collisional regime has been correlated to the ability of the lattice to accommodate the formation of Frenkel pairs by site exchange [18]. Compounds with a high ratio of cation radii get amorphized because vacancies and interstitials accumulate instead of recombining at random. At thermodynamic equilibrium also, the closer the ratio of cation radii is to 1, the lower is the temperature of the transformation ($T_{OD}$) from pyrochlore to anion-deficient fluorite structure (Table 1) [20,21]. Conversely pyrochlores with high ordering tendency such as $Gd_2Ti_2O_7$ are stable up to the melt [10].

It is known that SHI passing through materials induce a high density of electronic excitations and ionizations in a narrow cylinder and that the system relaxes within a short time (some fraction of nano seconds) by different processes depending on the nature of bonds. The most general relaxation process is a strong agitation of the atomic lattice resulting from a transfer of the electrons energy by electron–phonon coupling. The temperature may reach several thousand Kelvin and, since this thermal spike is quenched at high rate, one can easily understand that the high temperature solid phase (anion-deficient fluorite) is formed when the disorder of the melt phase can be accommodated by antisite formation in the lattice. On the contrary in the case of compounds with a high tendency to ordering at equilibrium, the disorder of the melt remains frozen for kinetic reasons.

The radiation resistance in nuclear regime shows a strong correlation with the ionicity of bonds as discussed in [22,23]. Computations of electronic structures indicate a slightly lower ionicity of the Ti–O bonds in $TiO_2$ than for Zr–O in $ZrO_2$, which may explain the stronger resistance of both $ZrO_2$ and $Gd_2Zr_2O_7$ to damaging by cascades than of $TiO_2$ and $Gd_2Ti_2O_7$ [22,23]. Nevertheless, the ionicity of A–O and B–O bonds in complex oxides ABO are not independent as shown for instance by the study of Lian [24,25], so that the criterion proposed by Trachenko is debatable. In addition, many ionic compounds which are strongly resistant to the chemical disordering by cascades ($MgAl_2O_4$, $Si_3N_4$) are highly sensitive to the topological disordering by thermal spikes and, reversely, covalent semiconductors such as SiC are extremely resistant to thermal spikes [26]. Other factors have to be considered such as the thermal conductivity, electron–phonon coupling constant or electron mean free path, melting temperature.

Thus, the correlation of the radiation resistance with the energy required for the formation of cation antisites and anion Frenkel pairs, proposed by Sickafus et al. for the damaging in nuclear stopping regime [18,19] appears also very relevant in the electronic stopping regime.

Finally one more interesting observation, comparing the results in the available literature, is that even though the mode of energy transferred to these pyrochlores is different, i.e. be it low energy [10] or high energy ions (Present work) or simply increase in the temperature [20] or even recently reported, increase in the hydrostatic pressure [27,28] the transformations occurring are the same.

From these measurements, the threshold in the $S_e$ ($S_{eth}$) required to amorphize $Gd_2Zr_2O_7$ is greater than 22.2 keV/nm. From Fig. 2 the $S_{eth}$ for $Nd_2Zr_2O_7$ appears to be between 16 and 20 keV/nm, while that for $Gd_2Ti_2O_7$ appears much lower than 11.8 keV/nm. It follows from the above discussion that $Gd_2Zr_2O_7$ is less susceptible to damaging by FF and in fact a small amount of recrystallization was also observed upon increase in the fluence from $5 \times 10^{17}$ to $1 \times 10^{18}$ ions/$m^2$. In fact in a parallel irradiation study by Thomé and co-workers [29] of CSNSM, Orsay with 1.5 GeV Xe ions show that there is no amorphization of $Gd_2Zr_2O_7$ and the $S_e$ in this case was above 35 keV/nm. Hence, it is a potential candidate as host lattice for the incorporation of MA to be transmuted in the present reactors or futuristic accelerator driven sub-critical systems.

## 4. Conclusions

The radiation stability of three pyrochlores under SHI irradiation was studied. XRD and Raman investigations confirm the pyrochlore to anion-deficient fluorite transformation in $Gd_2Zr_2O_7$

and $Nd_2Zr_2O_7$. Amorphization was observed in $Gd_2Ti_2O_7$ at the lowest $S_e$ employed. The correlation between the resistance to amorphization and ratio of cations radii (defining the formation energy of cation antisites) appears a suitable criterion in the electronic stopping regime of ions also. The present work indicates that pyrochlores with $r_A/r_B$ on the borderline of phase transformation between ordered pyrochlore and anion-deficient fluorite, like $Gd_2Zr_2O_7$ are favorable candidates for IMF.

## Acknowledgments

This work was carried out at the IUAC under the beamtime request, BTR No. 38103 MS. We also acknowledge DST for providing funds for XRD system at IUAC under the IRPHA project and Dr Foran Singh for the Raman measurements. The first author acknowledges the Fellowship provided by Department of Atomic Energy, India under the Mumbai University-BARC colloborative scheme and the French embassy, India under the Sandwich PhD program.

## References

[1] R.C. Ewing, Proc. Natl. Acad. Sci. USA 96 (1999) 3432.
[2] R.C. Ewing, W.J. Weber, F.W. Clinard, Progr. Nucl. Energy 29 (1995) 63.
[3] Hj. Matzke, V.V. Rondinella, T. Wiss, J. Nucl. Mater. 274 (1999) 47.
[4] M. Burghartz, Hj. Matzke, C. Léger, G. Vambernepe, M. Rome, J. Alloys Compd. 271–273 (1998) 544.
[5] M. Toulemonde, Ch. Dudour, A. Meftah, E. Paumier, Nucl. Instrum. and Meth. B 166&167 (2000) 903.
[6] H. Dammak, A. Barbu, A. Dunlop, D. Lesueuer, N. Lorenzelli, Philos. Mag. Lett. 67A (1993) 256.
[7] Abdenacer Benyagoub, Phys. Rev. B 72 (2005) 094114.
[8] A. Meftah, F. Brisard, J.M. Costantini, E. Dooryhee, M. Hage Ali, M. Hervieu, J.P. Stoquert, F. Studer, M. Toulemonde, Phys. Rev. B 49 (1994) 12457.
[9] S. Lutique, D. Staicu, R.J.M. Konings, V.V. Rondinella, J. Somers, T. Wiss, J. Nucl. Mater. 319 (2003) 59.
[10] R.C. Ewing, W.J. Weber, J. Lian, J. Appl. Phys. 95 (2004).
[11] M. Beauvy, C. Dalmasso, C. Thiriet-Dodane, D. Simeone, D. Gosset, Nucl. Instrum. and Meth. B 242 (2006) 557.
[12] J.F. Ziegler, J.P. Biersack, U. Littmark, The Stopping and Range of Ions in Solids, Pergamon, New York, 1985.
[13] M.A. Subramanian, G. Aravamudan, G.V. Subba Rao, Prog. Solid State Chem. 15 (1983) 55.
[14] M.J.D. Rushton, C.R. Stanek, A.R. Cleave, B.P. Uberuaga, K.E. Sickafus, R.W. Grimes, Nucl. Instrum. and Meth. B 255 (2007) 151.
[15] S. Bhagavantam, T. Venkataryudu, Proc. Indian Acad. Sci. 19 (1939) 224.
[16] M. Mori, G.M. Tompsett, N.M. Sammes, E. Suda, Y. Takeda, Solid State Ionics 158 (2003) 79.
[17] M. Glerup, O.F. Nielsen, T.W. Poulsen, J. Solid State Chem. 160 (2003) 25.
[18] K.E. Sickafus, R.W. Grimes, J.A. Valdez, A. Cleave, M. Tang, M. Ishimaru, S.M. Corish, C.R. Stanek, B.P. Uberuaga, Nature Mater. 6 (2007) 217.
[19] K.E. Sickafus, L. Minervini, R.W. Grimes, J.A. Valdez, M. Ishimaru, F. Li, K.J. McClellan, T. Harimann, Science 289 (2000) 748.
[20] D. Michel, M. Perez, Y. Jorba, R. Collongues, J. Raman Spectrosc. 5 (1976) 163.
[21] M.J.D. Rushton, R.W. Grimes, C.R. Stanek, S. Owens, J. Mater. Res. 19 (2004) 1603.
[22] K. Trachenko, J. Phys.: Cond. Matter 16 (2004) R1491.
[23] K. Trachenko, J.M. Pruneda, E. Artacho, M.T. Dove, Phys. Rev. B 71 (2005) 184104.
[24] J. Lian, J. Chen, L.M. Wang, R.C. Ewing, J.M. Farmer, L.A. Boatner, K.B. Helean, Phys. Rev. B 68 (2003) 134107.
[25] J. Lian, R.C. Ewing, L.M. Wang, K.B. Helean, J. Mater. Res. 19 (2004) 1575.
[26] S.J. Zinkle, J.W. Jones, V.A. Skuratov, MRS Proc. 540 (1999) 299.
[27] F.X. Zhang, J. Lian, U. Becker, R.C. Ewing, Jingzhu Hu, S.K. Saxena, Phys. Rev. B 76 (2007) 214104.
[28] F.X. Zhang, J.W. Wang, J. Lian, M.K. Lang, U. Becker, R.C. Ewing, Phys. Rev. Lett. 100 (2008) 045503.
[29] G. Sattonnay, S. Moll, L. Thomé, C. Legros, M. Herbst-Ghysel, F. Garrido, J.-M. Costantini, C. Trautmann, Nucl. Instrum. and Meth. B 266 (2008) 3043.